ELSEVIER

www.elsevier.nl/locate/carres

Carbohydrate Research 329 (2000) 847–853

CARBOHYDRATE RESEARCH

Complexation of trivalent lanthanide cations by inositols in the solid state: crystal structure and an FT-IR study of $PrCl_3 \cdot myo$-inositol$\cdot 9\ H_2O$

Limin Yang, Zheming Wang, Ying Zhao, Wen Tian, Yizhuang Xu, Shifu Weng, Jinguang Wu *

College of Chemistry and Molecular Engineering, Peking University, The University of Hong Kong Joint Laboratory in Rare Earth Materials and Bioinorganic Chemistry, Peking University, Beijing 100871, PR China

Received 4 May 2000; accepted 19 July 2000

Abstract

The title compound, $PrCl_3 \cdot C_6H_{12}O_6 \cdot 9\ H_2O$ crystallized in the monoclinic space group $P2_1/n$ with cell dimensions $a = 15.8293(3)$, $b = 8.67750(10)$, $c = 16.2292(3)$ Å, $\beta = 107.0788(8)°$, $V = 2130.92(6)$ Å^3 and $Z = 4$. Each Pr ion is coordinated to nine oxygen atoms, two from the inositol and seven from water molecules, with Pr–O distances from 2.4729 to 2.6899 Å; the other two water molecules are hydrogen-bonded. No direct contacts exist between Pr and Cl. There is an extensive network of hydrogen bonds formed by hydroxyl groups, water molecules, and chloride ions. The IR spectra of Pr–, Nd–, and Sm–inositol complexes are similar, which shows that the three metal ions have the same coordination mode. The IR results are consistent with the crystal structure.

Keywords: Lanthanide; Crystal structures; Complexation; *myo*-Inositol; FT-IR

1. Introduction

The interactions between metal ions and sugars are important in terms of biological activity [1–7], and their study can improve the understanding of interactions between metal ions and sugar residues of biologically important compounds [8–13].

Lanthanide complexes are often used as shift reagents to probe calcium binding-sites in aqueous solution. Rare earth ions, although biologically unnecessary, have biological effects of medical significance [14–20]. *myo*-Inositol, a naturally occuring inositol and found in all plant or animal tissues, was chosen as a model for investigating the coordination of rare earth ions with sugars. Inositols are essential growth factors for rapidly dividing cells, and a simple polyol precursor in a second messenger system is important in the brain [21,22].

Crystal structures are generally investigated in reference to solution studies. It is very probable that the main binding-sites are the same in the crystal and in solution. The synthesis and isolation of solid or crystalline metal–sugar complexes are hampered because complexes of neutral saccharides are weak owing to the high pK_a values of the hydroxyl groups ($pK_a > 12$) [23]. To date there is only

* Corresponding author. Fax: +86-10-6751708.
E-mail address: wjg@chemms.chem.pku.edu.cn (J. Wu).

0008-6215/00/$ - see front matter
PII: S0008-6215(00)00230-5

one reported crystal structure of a lanthanide–sugar complex ($2PrCl_3 \cdot$galactitol$\cdot 14\ H_2O$) [24]. The crystal structures of Sr–*epi*-inositol, Ca–*myo*-inositol and Mg–*myo*-inositol have been determined [25–27]. IR is also an important technique for studying the formation of metal–sugar complexes [28–32]. Here we report the crystal structure of Pr–*myo*-inositol and the IR spectra of Pr–, Nd–, and Sm–inositol. The IR spectra of Nd– and Sm–inositol are similar to Pr–inositol, showing that the same coordination mode occurs in the structures of Nd– and Sm–inositol. The IR spectra are consistent with the solid-state structures.

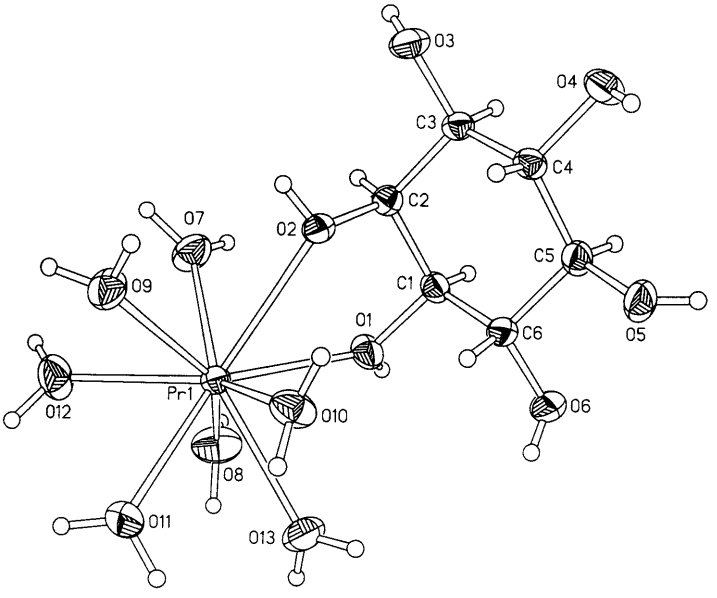

Fig. 1. Structure and atom numbering scheme of $PrCl_3 \cdot C_6H_{12}O_6 \cdot 9\ H_2O$.

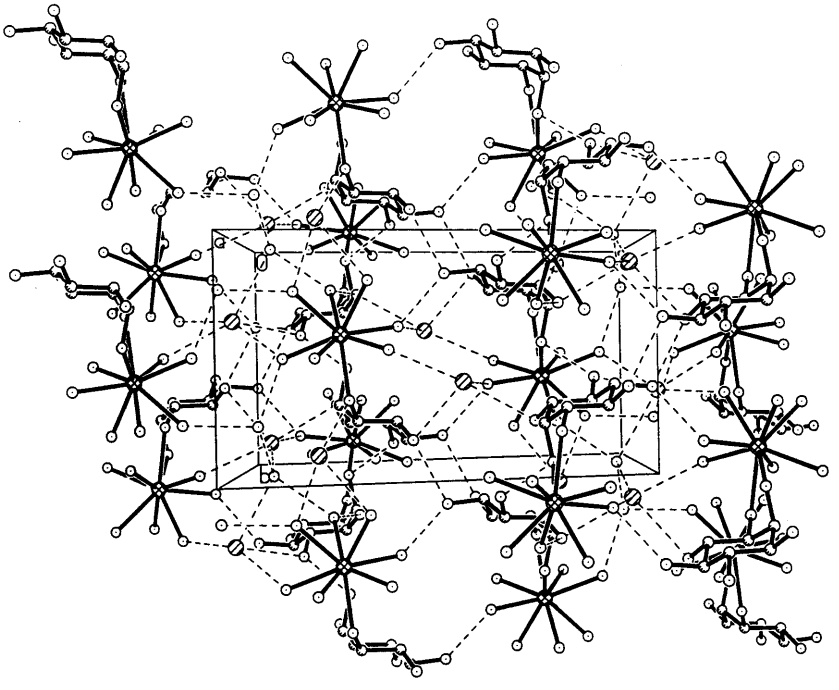

Fig. 2. Projection of the crystal cell in the structure of $PrCl_3 \cdot C_6H_{12}O_6 \cdot 9\ H_2O$.

Table 1
Crystal data for $PrCl_3 \cdot C_6H_{12}O_6 \cdot 9\ H_2O$

Formula	$PrCl_3 \cdot C_6H_{12}O_6 \cdot 9\ H_2O$
Formula weight	589.56
Space group	$P2_1/n$
a (Å)	15.8293(3)
b (Å)	8.67750(10)
c (Å)	16.2292(3)
β (°)	107.0788(8)
V (Å^3)	2130.92(6)
Z	4
D_{calcd} (Mg m^{-3})	1.838
Absorption coefficient (mm^{-1})	2.724
$F(000)$	1184
Crystal shape	block
Crystal color	light green
Crystal size (mm)	$0.28 \times 0.25 \times 0.17$
Refinement method	full-matrix least-squares on F^2
Goodness-of-fit on F^2	1.038
Final R indices [$I > 2\theta(I)$]	$R_1 = 0.0279$, $wR_2 = 0.0656$
R indices (all data)	$R_1 = 0.0390$, $wR_2 = 0.0694$
Data/restraints/parameters	6074/33/330

Table 2
Atomic coordinates ($\times 10^4$) and equivalent isotropic displacement parameters (Å$^2 \times 10^3$) for $PrCl_3 \cdot C_6H_{12}O_6 \cdot 9\ H_2O$

	x	y	z	U_{eq} [a]
Pr-1	5346(1)	4027(1)	2489(1)	19(1)
Cl-1	6920(1)	6650(1)	313(1)	45(1)
Cl-2	6513(1)	9122(1)	1995(1)	39(1)
Cl-3	6733(1)	6134(1)	5480(1)	42(1)
C-1	4720(2)	7815(3)	2863(2)	22(1)
C-2	3834(2)	7133(3)	2369(2)	20(1)
C-3	3080(2)	7947(3)	2598(1)	20(1)
C-4	3204(2)	8026(3)	3559(2)	21(1)
C-5	4105(2)	8707(3)	4046(2)	23(1)
C-6	4861(2)	7860(3)	3835(2)	23(1)
O-1	5391(1)	6883(2)	2686(1)	28(1)
O-2	3875(1)	5510(2)	2554(1)	22(1)
O-3	2268(1)	7161(2)	2210(1)	28(1)
O-4	2515(1)	8985(2)	3672(1)	31(1)
O-5	4214(1)	8567(2)	4947(1)	31(1)
O-6	5671(1)	8645(2)	4233(1)	33(1)
O-7	4591(1)	5043(2)	1022(1)	36(1)
O-8	6538(1)	5034(3)	1928(1)	42(1)
O-9	4170(1)	2049(2)	2198(1)	34(1)
O-10	5013(1)	3696(2)	3889(1)	33(1)
O-11	6207(1)	1739(2)	3197(1)	41(1)
O-12	5482(2)	2157(2)	1361(1)	39(1)
O-13	6718(1)	4724(3)	3694(1)	39(1)
O-14	4827(2)	7946(3)	430(1)	43(1)
O-15	3646(2)	201(3)	696(2)	50(1)

[a] U_{eq} is defined as one third of the trace of the orthogonalized U_{ij} tensor.

2. Results and discussion

The crystal structure of $PrCl_3 \cdot C_6H_{12}O_6 \cdot 9\ H_2O$ is shown in Fig. 1, and Fig. 2 is the projection of the crystal cell. Crystal data are listed in Table 1. Atomic coordinates and equivalent isotropic displacement parameters are listed in Table 2. Selected bond lengths and angles are collected in Table 3.

Each Pr ion is coordinated to nine oxygen atoms, two from the alditol (two adjacent hydroxyl groups) and seven from water molecules in a tricapped trigonal prism geometry, with Pr–O distances ranging from 2.4729 to 2.6899 Å; the other two water molecules are hydrogen-bonded (Table 3). No direct contacts exist between Pr and Cl. The crystal structures of Ca–*myo*-inositol and Mg–*myo*-inositol have been published [26,27]. For $CaBr_2$–*myo*-inositol·5 H_2O, the calcium ion binds to two symmetry-related molecules and four water molecules. One *myo*-inositol molecule chelates the calcium ion through its 2- and 3-hydroxyl groups, and the second *myo*-inositol molecule chelates the calcium ion through its 5- and 6-hydroxyl groups, the eight oxygen atoms form a distorted square-antiprism with calcium–oxygen distances ranging from 2.37 to 2.52 Å [26]. For $MgCl_2$–*myo*-inositol·4 H_2O, the magnesium ion is coordinated to the cis vicinal hydroxyl oxygens at positions 1 and 2 and four water molecules in an octahedral geometry [27]. The uncharged sugar chelates metal ions through pairs of adjacent hydroxyl groups, and the coordination of Mg is closer to that of rare earth ions. In the coordination sphere of rare earth ions there are more water molecules, and the coordination number is higher. The difference in coordination modes stems from the difference of radius and charge between rare earth ions and alkaline earth ions. More hydrogen bonds exist in the crystal structures of the rare earth complex for the same reason. There are extensive networks of hydrogen bonds formed between hydroxyl groups, water molecules, and chloride ions in the crystal structure of the lanthanide complex.

For Pr–inositol, Cl-1 is involved in hydrogen bonding with six atoms: O-4, O-7, O-8, O-11, O-14, and O-15; Cl-2 is related to the

following atoms through hydrogen bonding: O-1, O-8, O-11, O-12, O-13, and O-14; and Cl-3 links to five atoms by hydrogen bonding: O-3, O-6, O-10, O-13, and O-15. Two water molecules (O-14 and O-15) do not coordinate with the metal ion and are hydrogen-bonded. For O-14, the following hydrogen-bonds appear: O-14–H-27···O-15 (x, $y+1$, z); O-14–H-28···Cl-2; O-14–H-28···Cl-1; O-7–H-13···O-14; O-12–H-24···O-14 ($-x+1$, $-y+1$, $-z$). O-15 hydrogen bonds with four atoms: O-15–H-29···Cl-1 ($-x+1$, $-y+1$, $-z$); O-15–H-30···Cl-3 ($x-1/2$, $-y+1/2$, $z-1/2$); O-14–H-27···O-15 (x, $y+1$, z); O-9–H-18···O-15. For the inositol, every OH group is hydrogen bonded with another atom, four of them chlorides and two hydroxyl groups of another inositol molecule (Table 4). Metal–hydroxyl interactions generally produce small conformational changes in the sugar at the metal-binding sites. Comparing uncomplexed *myo*-inositol with the Pr–inositol complex, the C–C and C–O distances and bond angles show only small changes [33], and the chair conformation of inositol is maintained in the complex structures (Fig. 2), as with the Ca– or Mg–complexes [26,27]. Minor differences are reflected in the IR spectra, which are discussed later. In aqueous solution the NMR spectrum of *myo*-inositol shows no substantial changes on addition of cations, and metal–*myo*-inositol complexes show very little mobility on electrophoresis [34–36]. The characteristic colors of Pr–, Nd– and Sm–inositol compounds are light green, purple and yellow, respectively.

Table 3
Selected bond lengths (Å) and angles (°) for $PrCl_3{\cdot}C_6H_{12}O_6{\cdot}9H_2O$

Bond lengths			
Pr-1–O-9	2.4729(19)	C-1–C-6	1.528(3)
Pr-1–O-8	2.4832(19)	C-2–O-2	1.437(3)
Pr-1–O-7	2.4894(19)	C-2–C-3	1.524(3)
Pr-1–O-11	2.490(2)	C-3–O-3	1.428(3)
Pr-1–O-10	2.4963(18)	C-3–C-4	1.515(3)
Pr-1–O-1	2.4976(19)	C-4–O-4	1.426(3)
Pr-1–O-12	2.5018(19)	C-4–C-5	1.532(3)
Pr-1–O-13	2.5322(19)	C-5–O-5	1.427(3)
Pr-1–O-2	2.6899(17)	C-5–C-6	1.526(3)
C-1–O-1	1.430(3)	C-6–O-6	1.428(3)
C-1–C-2	1.516(3)		
Bond angles			
O-9–Pr-1–O-8	141.69(7)	O-9–Pr-1–O-2	74.21(6)
O-9–Pr-1–O-7	86.57(7)	O-8–Pr-1–O-2	127.30(7)
O-8–Pr-1–O-7	74.20(7)	O-7–Pr-1–O-2	71.95(6)
O-9–Pr-1–O-11	79.30(7)	O-11–Pr-1–O-2	136.59(7)
O-8–Pr-1–O-11	94.46(8)	O-10–Pr-1–O-2	66.59(6)
O-7–Pr-1–O-11	140.13(7)	O-1–Pr-1–O-2	60.83(5)
O-9–Pr-1–O-10	75.28(7)	O-12–Pr-1–O-2	126.93(6)
O-8–Pr-1–O-10	139.55(7)	O-13–Pr-1–O-2	114.29(6)
O-7–Pr-1–O-10	137.81(7)	O-1–C-1–C-2	107.45(19)
O-11–Pr-1–O-10	73.82(7)	O-1–C-1–C-6	109.26(19)
O-9–Pr-1–O-1	134.82(6)	C-2–C-1–C-6	112.86(19)
O-8–Pr-1–O-1	72.63(7)	O-2–C-2–C-1	107.10(19)
O-7–Pr-1–O-1	76.04(7)	O-2–C-2–C-3	113.15(18)
O-11–Pr-1–O-1	137.80(7)	C-1–C-2–C-3	111.01(19)
O-10–Pr-1–O-1	90.18(7)	O-3–C-3–C-4	107.62(19)
O-9–Pr-1–O-12	68.42(7)	O-3–C-3–C-2	109.82(19)
O-8–Pr-1–O-12	73.84(8)	C-4–C-3–C-2	113.49(19)
O-7–Pr-1–O-12	69.56(7)	O-4–C-4–C-3	106.61(19)
O-11–Pr-1–O-12	70.57(7)	O-4–C-4–C-5	109.9(2)
O-10–Pr-1–O-12	132.70(7)	C-3–C-4–C-5	111.55(19)
O-1–Pr-1–O-12	137.05(7)	O-5–C-5–C-6	108.8(2)
O-9–Pr-1–O-13	137.73(7)	O-5–C-5–C-4	108.0(2)
O-8–Pr-1–O-13	68.12(7)	C-6–C-5–C-4	111.78(19)
O-7–Pr-1–O-13	135.68(7)	O-6–C-6–C-5	109.1(2)
O-11–Pr-1–O-13	66.72(8)	O-6–C-6–C-1	108.6(2)
O-10–Pr-1–O-13	71.74(7)	C-5–C-6–C-1	110.96(19)
O-1–Pr-1–O-13	71.22(7)	C-1–O-1–Pr-1	126.26(14)
O-12–Pr-1–O-13	118.75(7)	C-2–O-2–Pr-1	116.53(13)

The FT-IR spectral data and possible assignments in the 1500–650 cm^{-1} region are listed in Table 5; spectra are shown in Fig. 3. In the 4000–3000 cm^{-1} region, the stretching vibration peaks of the OH groups in the three spectra are broadened as compared with the spectrum of the free inositol. A strong and broad peak could be assigned to hydroxyl stretching vibrations of the inositol, and the water OH stretching vibration is influenced by the extensive hydrogen-bonding network. Complexation changes and broadens the inositol peak positions in this region. The spectrum of $PrCl_3{\cdot}$*myo*-inositol$\cdot 9\,H_2O$ cooled to liquid N_2 temperature, recorded by the Nujol mull method (Fig. 4), is difficult to assign in detail. The eight low frequency peaks (3159–3372 cm^{-1}) may be assigned to O–H···O stretching vibrations, assuming that ν(OH) is primarily related to the O···O distance d(O···O). The shorter d(O···O) is, the larger is the effect on the OH stretching vibration, and the lower ν(OH) [37]. The peaks at higher frequencies may be related to O–H···Cl vibrations.

Table 4
Hydrogen bonds for $PrCl_3 \cdot C_6H_{12}O_6 \cdot 9\ H_2O$ [a]

D–H···A	d(D–H)	d(H···A)	d(D···A)	<(DHA)
O-1–H-7···Cl-2	0.801(18)	2.272(19)	3.058(2)	167(3)
O-2–H-8···O-4 #1	0.793(18)	2.033(19)	2.824(3)	175(3)
O-3–H-9···Cl-3 #2	0.812(18)	2.28(2)	3.065(2)	162(4)
O-4–H-10···Cl-1 #3	0.821(19)	2.36(3)	3.123(2)	155(4)
O-5–H-11···O-6 #4	0.806(18)	1.936(18)	2.741(3)	178(3)
O-6–H-12···Cl-3	0.801(18)	2.313(18)	3.110(2)	173(3)
O-7–H-13···O-14	0.930(18)	1.831(18)	2.760(3)	179(5)
O-7–H-14···Cl-1 #5	0.926(18)	2.164(19)	3.087(2)	174(4)
O-8–H-15···Cl-1	0.930(18)	2.28(2)	3.183(2)	162(3)
O-8–H-16···Cl-2 #6	0.928(18)	2.240(18)	3.168(2)	179(4)
O-9–H-17···O-3 #1	0.925(18)	1.804(19)	2.720(2)	170(4)
O-9–H-17···O-4 #1	0.925(18)	2.63(4)	3.117(3)	114(3)
O-9–H-18···O-15	0.929(18)	1.91(2)	2.831(3)	173(4)
O-10–H-19···Cl-3 #7	0.916(18)	2.35(2)	3.220(2)	160(3)
O-10–H-20···O-5 #7	0.933(18)	1.822(19)	2.750(3)	173(4)
O-11–H-21···Cl-1 #6	0.920(18)	2.35(2)	3.230(2)	160(3)
O-11–H-22···Cl-2 #8	0.899(18)	2.24(2)	3.123(2)	167(4)
O-12–H-23···Cl-2 #8	0.921(18)	2.194(18)	3.110(2)	173(4)
O-12–H-24···O-14 #5	0.930(18)	1.90(2)	2.804(3)	164(4)
O-13–H-25···Cl-3	0.933(18)	2.22(2)	3.140(2)	171(4)
O-13–H-26···Cl-2 #6	0.915(18)	2.51(2)	3.348(2)	152(3)
O-14–H-27···O-15 #9	0.940(18)	1.904(19)	2.825(3)	166(4)
O-14–H-28···Cl-2	0.939(18)	2.46(3)	3.261(2)	143(3)
O-14–H-28···Cl-1	0.939(18)	2.91(3)	3.557(3)	127(3)
O-15–H-29···Cl-1 #5	0.938(18)	2.25(2)	3.176(3)	169(4)
O-15–H-30···Cl-3 #10	0.917(18)	2.25(2)	3.164(2)	174(3)

[a] Symmetry transformations used to generate equivalent atoms: (#1) $-x+1/2, y-1/2, -z+1/2$; (#2) $x-1/2, -y+3/2, z-1/2$; (#3) $x-1/2, -y+3/2, z+1/2$; (#4) $-x+1, -y+2, -z+1$; (#5) $-x+1, -y+1, -z$; (#6) $-x+3/2, y-1/2, -z+1/2$; (#7) $-x+1, -y+1, -z+1$; (#8) $x, y-1, z$; (#9) $x, y+1, z$; (#10) $x-1/2, -y+1/2, z-1/2$.

In the 3000–2000 cm^{-1} region, the weak peaks could be assigned to CH stretching vibrations (2936, 2930, 2899, and 2812 cm^{-1} for Pr–inositol, 2937, 2899, 2874, and 2811 cm^{-1} for Nd–inositol, and 2938, 2930, 2899, 2874, and 2816 cm^{-1} for Sm–inositol) [38]. When the metal complexes are formed, the relative intensities of the CH stretching vibrations are clearly decreased and the peak positions are shifted in the spectra of the metal complexes. M–O band formation changes the CH stretching vibrations, and the OH vibrations have mask the CH bands.

In the 1700–1500 cm^{-1} region, the medium bands at $\sim 1640\ cm^{-1}$, which are absent from the spectrum of the free inositol, are assigned to deformation vibrations of water molecules. Two peaks (1642 and 1621 cm^{-1} for Pr–inositol, 1642 and 1622 cm^{-1} for Nd–inositol, and 1644 and 1623 cm^{-1} for Sm–inositol) appear in the region. The relative intensities of the ~ 1644 and $\sim 1623\ cm^{-1}$ bands among the three spectra are the largest in the Sm–inositol spectrum and the relative intensity in the Nd–inositol spectrum is larger than for Pr–inositol; this is probably related to the different M–O distances. The appearance of some shoulder peaks may have the same reason. The curvefit result for Pr–inositol is shown in Fig. 5. The two peaks could be split into nine peaks, corresponding to different water molecules.

The 1500–650 cm^{-1} region, 1500–1200 cm^{-1} for the sugar itself may be called the local symmetry region, because it is mainly constituted of the deformational vibrations of groups having local symmetry, such as HCH, and the vibrations of the CH_2OH group. The 1200–950 cm^{-1} region is the CO stretching region and 950–700 cm^{-1} the side-groups deformational-region (COH, CCH, OCH); this includes the important fingerprint or anomeric bands between 930 and 840 cm^{-1}, and an appreciable contribution from the stretching of C–C; 700–500 cm^{-1}, and exocyclic deformations (CCO, CCC, COH) [39]. Each peak exhibits coupling by many vibration modes. As compared with the spectrum of inositol, the peak positions and relative intensities of the peaks are changed in the spectra of the metal complexes. Their spectra in this region are similar, showing that the three rare earth ions have the same coordination mode. This is comparable with our results on galactitol complexes of Pr, Nd, and Sm and it illustrates that ligands coordinate to light rare earth ions in the same way because of the similarity among light rare earth ions in radius and charge. The differences of 0–2 cm^{-1} show the characteristics of each metal ion coordination (Table 5).

In conclusion, IR reflects minor differences in the structures and it is a useful technique for studying complex formation.

Table 5
IR data for *myo*-inositol and its Pr–, Nd–, and Sm–complexes (1500–650 cm^{-1})

inositol	Pr–inositol	Nd–inositol	Sm–inositol	Preliminary assignment [30–32,39]
1446	1431	1431	1433	ν(CC), ν(CO), δ(COH)
1417	1396	1397	1396	ν(CC), ν(CO), δ(CCO), δ(COH), τ(CCCH)
1371	1373	1374	1374	ν(CC), δ(CCH), δ(COH), τ(CCCH)
1356	1348	1347	1349	ν(CC), δ(CCO), δ(CCH), δ(COH), τ(CCCH)
1324	1325	1325	1325	δ(COH), τ(CCCH), ν(CO), δ(CCH)
1273	1271	1272	1271	δ(COH), ν(CO), τ(CCCO), ν(CC)
1246	1259	1259	1259	
	1240	1240	1242	δ(COH)
1220		1225	1225	ν(CO)
1196	1199	1199	1199	ν(CC), ν(CO), τ(CCCO)
1148	1152	1152	1152	ν(CO), τ(CCCC), τ(OCCC)
1115	1109	1109	1109	ν(CO), ν(CC)
	1092	1092	1091	ν(CO)
1052	1045	1045	1045	
1015	1006	1007	1006	ν(CC), ν(CO), τ(OCCC)
1002				
930		939	939	
899	870	870	872	ν(CC), τ(CCCC), τ(OCCC)
894				
733	744	745	746	ν(CH), δ(CCC), ν(CC), τ(OCCC)
	729	730	731	
670			716	ν(CC), ν(CH), τ(CCCC), τ(OCCC)

3. Experimental

Materials.—$NdCl_3$, $PrCl_3$, and $SmCl_3$ were prepared and crystallized from the corresponding rare earth oxide of high purity (99.99%). *myo*-Inositol (Certified Biological Reagent) was provided by EG Ltd, and was used as supplied.

Synthesis of metal complexes. The inositol and 1 equiv of metal chloride were dissolved in water–EtOH and heated to prepare a concentrated solution, which was cooled down for crystallization. Anal. Calcd for $PrCl_3 \cdot C_6H_{12}O_6 \cdot 9\,H_2O$: C, 12.22; H, 5.129. Found: C, 11.87; H, 5.131. Anal. Calcd for $NdCl_3 \cdot$

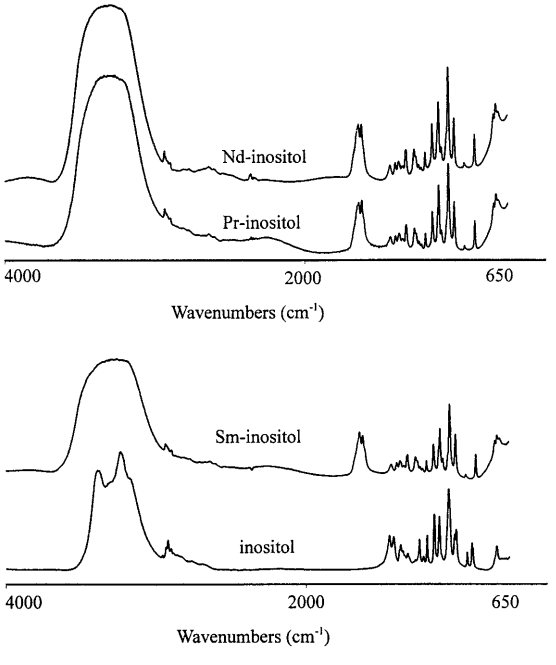

Fig. 3. Mid-IR spectra of *myo*-inositol and its Pr–, Nd–, and Sm–complexes.

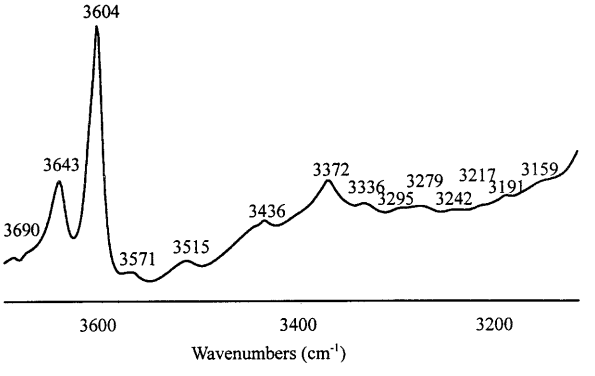

Fig. 4. The spectrum of Pr–*myo*-inositol on cooling to liquid N_2 temperature.

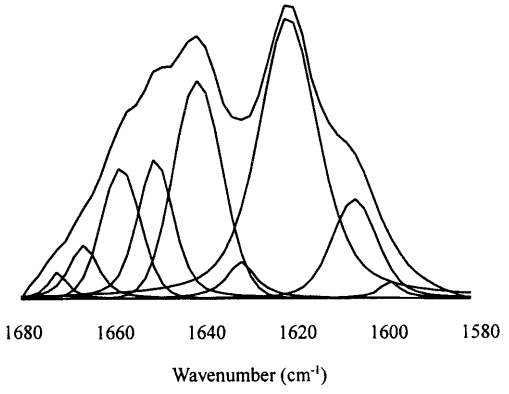

Fig. 5. The curvefit result for Pr–*myo*-inositol.

$C_6H_{12}O_6 \cdot 9\,H_2O$: C, 12.15; H, 5.100. Found: C, 11.31; H, 5.00. Anal. Calcd for $SmCl_3 \cdot C_6H_{12}O_6 \cdot 9\,H_2O$: C, 12.03; H, 5.048. Found: C, 11.92; H, 4.956.

Physical measurements. X-Ray diffraction data for $PrCl_3 \cdot$inositol$\cdot 9\,H_2O$ were measured on a Nonius Kappa CCD instrument, with Mo K_α radiation ($\lambda = 0.71073$ Å) in the θ range from 3.49 to 30.03° at 293(2) K. The final cycle of full-matrix least-squares refinement was based on 6074 observed reflections. Calculations were completed with SHELX-97 program. The three mid-IR spectra were measured on a Nicolet Magna-IR 750 spectrometer using micro-IR method, 128 scans at 4 cm^{-1} resolution.

Acknowledgements

The authors thank the National Natural Science Foundation of China for grants (Nos. 29671002 and 39730160) and the State Key Project for Fundamental Research of MOST (G1998061311) for supporting this work.

References

[1] L.N. Ji, *Bioinorganic chemistry*, Zhongshan University Press, 1995.
[2] J.A. Rendleman, Jr., *Adv. Carbohydr. Chem.*, 21 (1966) 209–271.
[3] S.J. Angyal, *Chem. Soc. Rev.*, 9 (1980) 415–428.
[4] Yu.E. Alekseev, A.D. Garnovskii, Yu.A. Zhdanov, *Usp. Khim.*, 67 (1998) 723–744.
[5] K. Burger, L. Nagy, *Biocoordination Chemistry: Coordination Equilibria in Biologically Active Systems*, 1990, pp. 236–283.
[6] J.F. Verchere, S. Chapelle, F. Xin, D.C. Crans, *Progr. Inorg. Chem.*, 47 (1998) 837–945.
[7] R.P. Bandwar, C.P. Rao, *Curr. Sci.*, 72 (1997) 788–796.
[8] H. Sigel, *Chem. Soc. Rev.*, 22 (1993) 255–267.
[9] D.M. Whitfield, S. Stojkovski, B. Sarkar, *Coord. Chem. Rev.*, 122 (1993) 171–225.
[10] S.J. Angyal, *Adv. Carbohydr. Chem. Biochem.*, 47 (1989) 1–43.
[11] S. Yano, M. Otsuka, in H. Sigel (Ed.), *Metal Ions in Biological Systems*, Vol. 32, 1996, pp. 27–60.
[12] S. Yano, *Coord. Chem. Rev.*, 92 (1988) 113–156.
[13] P. Umberto, F. Carlo, *Progr. Inorg. Chem.*, 46 (1997) 393–429.
[14] K Wang, *S. Afr. J. Chem.*, 50 (1997) 232.
[15] Y.J. Ji, Z.H. Wang, J.L. Li, S.H. Peng, *J. Health Toxicol.*, 8 (1994) 165.
[16] Y.Y. Song, Y.Z. Xu, S.F. Weng, L.B. Wang, X.F. Li, T.F. Zhang, J.G. Wu, *Biospectroscopy*, 5 (1999) 371–377.
[17] Y.Y. Song, X.F. Li, L.B. Wang, Y.Z. Xu, J.G. Wu, *Chin. J. Inorg. Chem.*, 15 (1999) 509–512.
[18] D.T. Xie, L.B. Wang, J.G. Wu, G.X. Xu, *J. Rare Earths*, 17 (1999) 81–82.
[19] J.Z. Ni, *Bioinorganic Chemistry of Lanthanides*, Science Press, Beijing, 1995.
[20] X.X. Gao, *The Application of Rare Earths in Agriculture and Electroanalysis Chemistry*, Peking University Press, Beijing, 1997.
[21] K. Othmer, *Encycl. Chem. Technol.*, 24 (1983) 50–58.
[22] T. Levine, *Eur. Neuropsychopharmacol.*, 7 (1997) 147–155.
[23] R.L. Lohmar, in W. Pigman (Ed.), *The Carbohydrates*, Academic Press, New York, 1957, p. 241.
[24] S.J. Angyal, D.C. Craig, *Carbohydr. Res.*, 241 (1993) 1–8.
[25] R.A. Wood, U.J. James, S.J. Angyal, *Acta Crystallogr., Sect. B*, 33 (1977) 2248–2251.
[26] W.J. Cook, C.E. Bugg, *Acta Crystallogr., Sect. B*, 29 (1973) 2404–2411.
[27] G. Blank, *Acta Crystallogr., Sect. B*, 29 (1973) 1677–1683.
[28] Y.M. Yang, S.F. Weng, J.G. Wu, G.X. Xu, *Chem. J. Chin. Univ.*, 15 (1994) 646–650.
[29] H. Liang, H. Guo, D.F. Xu, J.G. Wu, *Microchim. Acta*, I (1988) 215–217.
[30] L.Q. Yang, J.G. Wu, Q. Zhou, J. Bian, Y.M. Yang, D.F. Xu, G.X. Xu, *Microchim. Acta*, 14 (1997) 251–252.
[31] J.G. Wu, *Modern Fourier Transform Spectroscopic Techniques and Its Applications*, Science and Technology References Press, Beijing, 1994.
[32] W. Tian, L.M. Yang, Y.Z. Xu, S.F. Weng, J.G. Wu, *Carbohydr. Res.*, 324 (2000) 45–52.
[33] I.N. Rabinowitz, J. Kraut, *Acta Crystallogr.*, 17 (1964) 159–168.
[34] S.J. Angyal, D. Greeves, V.A. Pickles, *J. Chem. Soc., Chem. Commun.*, 1974, 589–590.
[35] S.J. Angyal, D. Greeves, *Aust. J. Chem.*, 29 (1976) 1223–1230.
[36] S.J. Angyal, R.J. Hickman, *Aust. J. Chem.*, 28 (1975) 1279–1287.
[37] E.T.G. Lutz, J.H. Van der Maas, *J. Mol. Struct.*, 324 (1994) 123–132.
[38] S. Pizzini, G. Bajo, S. Abbate, *Carbohydr. Res.*, 184 (1988) 1–11.
[39] M. Mathlouthi, J.L. Koenig, *Adv. Carbohydr. Chem. Biochem.*, 44 (1986) 7–89.